YALE
PEABODY
MUSEUM

P.O. BOX 208118 | NEW HAVEN CT 06520-8118 USA | PEABODY.YALE. EDU

Journal of Marine Research

The *Journal of Marine Research,* one of the oldest journals in American marine science, published important peer-reviewed original research on a broad array of topics in physical, biological, and chemical oceanography vital to the academic oceanographic community in the long and rich tradition of the Sears Foundation for Marine Research at Yale University.

An archive of all issues from 1937 to 2021 (Volume 1–79) are available through EliScholar, a digital platform for scholarly publishing provided by Yale University Library at https://elischolar.library.yale.edu/.

Requests for permission to clear rights for use of this content should be directed to the authors, their estates, or other representatives. The *Journal of Marine Research* has no contact information beyond the affiliations listed in the published articles. We ask that you provide attribution to the *Journal of Marine Research*.

Yale University provides access to these materials for educational and research purposes only. Copyright or other proprietary rights to content contained in this document may be held by individuals or entities other than, or in addition to, Yale University. You are solely responsible for determining the ownership of the copyright, and for obtaining permission for your intended use. Yale University makes no warranty that your distribution, reproduction, or other use of these materials will not infringe the rights of third parties.

This work is licensed under a Creative Commons Attribution-NonCommercial-ShareAlike 4.0 International License. https://creativecommons.org/licenses/by-nc-sa/4.0/

Journal of Marine Research, 68, 799–818, 2010

Investigation of the physicochemical features and mixing of East/Japan Sea Intermediate Water: An isopycnic analysis approach

by Il-Nam Kim[1], Dong-Ha Min[1], Dae Hyun Kim[2] and Tongsup Lee[3,4]

ABSTRACT

We present spatial distributions of the mixing ratio and properties of the East/Japan Sea Intermediate Water (ESIW) at its core density layer (σ_θ = 27.2–27.3) based on high-quality hydrographic data observed in the East/Japan Sea (EJS) during summer 1999. ESIW is defined as a source water type showing minimum salinity and maximum dissolved oxygen concentration. ESIW plays an important role in supplying dissolved oxygen and transporting anthropogenic carbon into the intermediate/deep layers in EJS. Studying the ESIW formation and distribution processes may provide insights on EJS's shallow- to mid-depth thermohaline circulation and recent ocean changes. Here, we combine the previously estimated mixing ratio of ESIW, based on Optimum Multi-Parameter (OMP) analysis, and its physicochemical properties, such as pressure, dissolved oxygen, and phosphate, interpolated onto several isopycnic surfaces (σ_θ = 27.20, 27.25, and 27.30). The physicochemical properties of ESIW show steep north-south gradients across the subpolar front at 40–41°N. Higher dissolved oxygen concentrations ($\geq$ 335 μmol kg^{-1}) of ESIW are found in the western Japan Basin particularly off the Primorye coast, indicating a potential source region. The spatial and depth distributions of apparent oxygen utilization (AOU) on the ESIW isopycnic surfaces indicate that the subduction of ESIW occurs at 131–133°E (Ulleung Basin) across the subpolar front to the south. The density layer of ESIW shoals near the Korean coast in the Ulleung Basin, implying a potential link to coastal upwelling. The relative age of ESIW at its core layer is estimated from the oxygen utilization rate and AOU. The correlation between the pCFC12 and relative ages, and AOU estimated at 90% surface water oxygen saturation condition suggests a decadal-scale ventilation of ESIW ($\leq$ 24 years). Younger waters at the ESIW coexist with the high-salinity intermediate water at the same density layer in the eastern Japan Basin. Our analysis suggests that ESIW is sensitive to climate forcing and an important shallow- to mid-depth thermohaline circulation component of EJS.

1. Introduction

The East/Japan Sea (EJS) is a semi-closed marginal sea (Fig. 1), but it exhibits many dynamics of the open oceans: deep-water formation, eddies, subpolar front, and gyre-like circulations. EJS is frequently referred as a "Miniature Ocean" (Lie and Seung, 1994;

1. Marine Science Institute, The University of Texas at Austin, Port Aransas, Texas, 78373, U.S.A.
2. Korea Inter-University Institute of Ocean Science, Pukyong National University, Busan, 608–737, Korea.
3. Division of Earth Environmental System, Pusan National University, Busan 609–735, Korea.
4. Corresponding author. ***email: tlee@pusan.ac.kr***

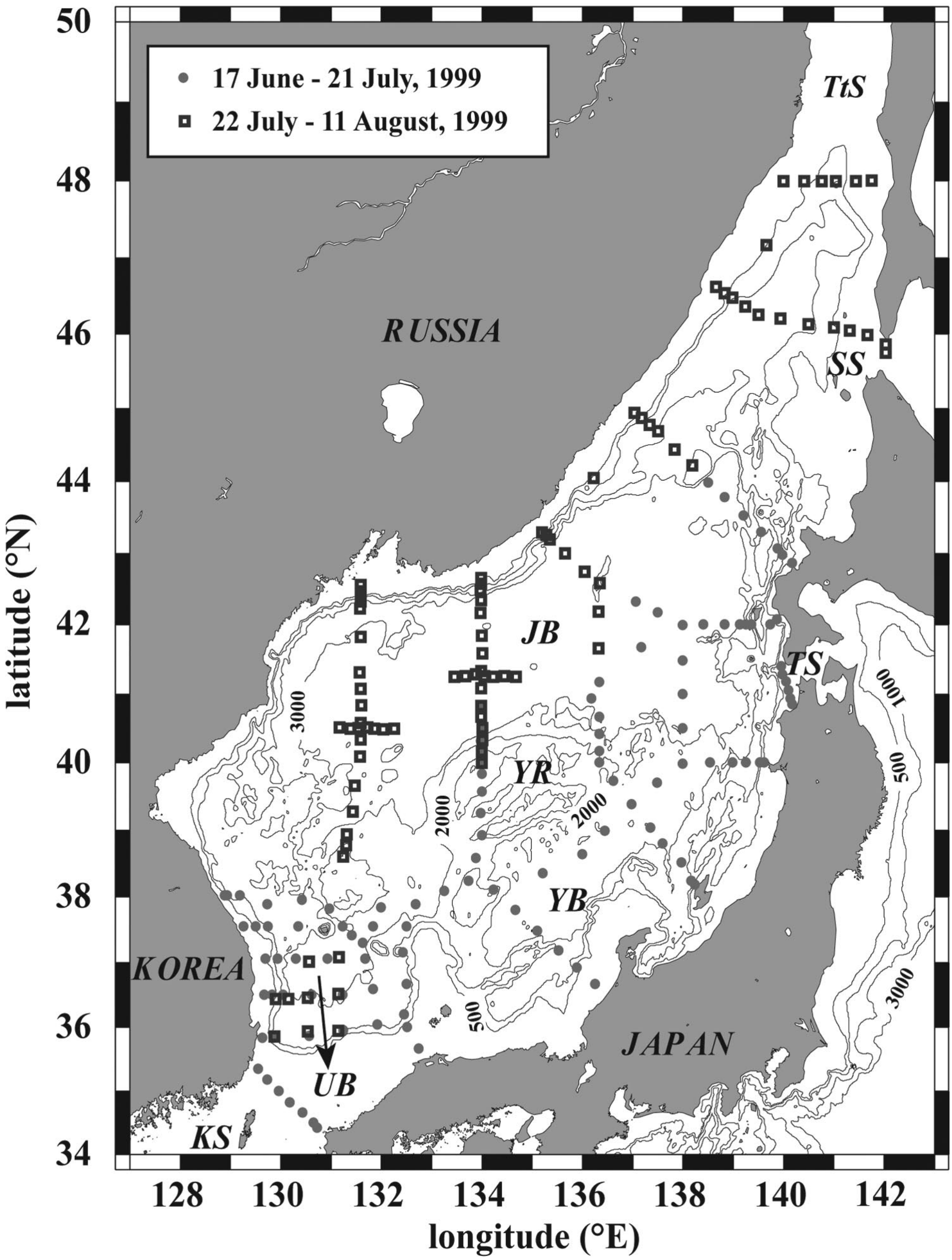

Figure 1. The study area map showing the 1999 summer CREAMS II hydrographic stations and the topography of the East/Japan Sea (EJS). The EJS shows dynamic topography that consists of three major basins; Japan basin (JB), Yamato Basin (YB), and Ulleung Basin (UB). Yamato Rise (YR) and four straits—Korea Strait (KS), Tsugaru Strait (TS), Soya Strait (SS), and Tatar Strait (TtS) are also marked on the map.

Gamo, 1999; Kim *et al.,* 2001; Min and Warner, 2005; Kim *et al.,* 2008). The surface layer of EJS is thermally divided into two regions by the subpolar front (~40°N). The southern EJS is dominated by warm subtropical waters, whereas the northern EJS is governed by cold subpolar waters. In winter, surface cooling by strong winds in the western Japan Basin (JB) is a key factor that drives the deep-water formation (Kim, K. *et al.,* 1991; Seung and Kim, 1993; Talley *et al.,* 2003). The ventilation of waters in the Ulleung and Yamato basins (UB and YB) depends largely on the deep-water formation in the western JB (WJB) accompanied with the supply of dissolved oxygen (DO).

The East/Japan Sea Intermediate Water (ESIW) has characteristics of a source water type showing minimum salinity and maximum dissolved oxygen. Its oxygen maximum feature is different from a typical oxygen minimum of other intermediate depth water masses, as ESIW exists at shallower depth layer. (Kim and Chung, 1984; Kim, K.-R. *et al.,* 1991). The ESIW plays an important role in supplying dissolved oxygen and transporting anthropogenic carbon into the intermediate/deep layers of EJS (Park *et al.,* 2006).

Recent studies of the EJS have reported changes in DO in intermediate and deep waters, claiming that the mode of deep water formation has been shifting from bottom to intermediate water formation mode due to global warming (Kim and Kim, 1996; Kim *et al.,* 2001; Kang *et al.,* 2003; Chae *et al.,* 2005). However, other studies reported sudden bottom-water formation in the northern EJS in winter 2000–2001 (Kim *et al.,* 2002; Senjyu *et al.,* 2002; Talley *et al.,* 2003; Tsunogai *et al.,* 2003). These facts imply that thermohaline circulation (THC) of EJS is sensitive to climate change. Thus, EJS is an ideal place to detect ocean changes caused by climate change due to its relatively short residence time scale of one hundred years (Kim *et al.,* 2001). The study of the ESIW formation and distribution processes can give insights on THC and its recent ocean change in EJS (Gamo, 1999; Kim *et al.,* 2001; Kim *et al.,* 2008).

ESIW was previously identified physicochemically with a subsurface salinity minimum and a DO maximum, with salinity < 34.06 psu, potential temperature > 1.0°C, and DO > 250 μmol l^{-1} (Kim and Chung, 1984; Kim. K.-R. *et al.,* 1991; Kim and Kim, 1999). It was also identified by a subsurface ^{3}H and ^{3}He extreme and a CFC maximum (Min and Warner, 2005; Postlethwaite *et al.,* 2005). ESIW originates in the northern JB along the Primorye coast of Russia according to numerical modeling studies (Yoshikawa *et al.,* 2001; Yoon and Kawamura, 2002). It is formed in WJB during winter (Seung, 1997; Kim and Seung, 1999; Kim *et al.,* 2004), and surface cooling and down-front wind driven by cold-air outbreaks play significant roles in initiating its subduction and formation (Lee *et al.,* 2006). The ESIW shows two different types (Talley *et al.,* 2006): a northern type, which is relatively fresher, warmer, lighter, and highly oxygenated, flows cyclonically along the subpolar front (Isobe and Isoda, 1997; Shin *et al.,* 2007); and a southern type showing opposite characteristics subducts across the subpolar front (40–41°N) and then spreads to UB (Shin *et al.,* 1998; Senjyu, 1999; Yoshikawa *et al.,* 1999; Min and Warner, 2005; Lee *et al.,* 2006; Shin, 2006; Shin *et al.,* 2007). The renewal time of ESIW is estimated at about 10 years (Seung and Kim, 1997) to 20.3–25.6 years (Yoshikawa *et al.,*

1999) from numerical modeling studies. Although our understanding of ESIW's formation, ventilation, characteristics, and origin have increased over the past two decades, spatial distributions of ESIW properties along its core density layer have not been fully analyzed yet.

Recently, Chen *et al.* (1999) and Kang *et al.* (2004) proposed that the bottom water of EJS may become anoxic during this century. The anoxic scenario implies that the ESIW's role of supplying oxygen into the interior of EJS will probably be affected significantly. Hence, understanding physicochemical properties of ESIW would be an important step to improve prediction of future EJS changes.

The main purposes of this study are to: (i) define the ESIW's core density layer based on its water mass mixing ratio, (ii) characterize and map the spatial distribution of physicochemical properties of the ESIW on its core isopycnal surfaces, (iii) infer the locations of formation and subduction of the ESIW, and (iv) estimate its relative and pCFC12 ages.

2. Data and methods

A basin-wide hydrographic investigation was carried out in EJS in summer 1999 through the CREAMS II program (Fig. 1). The first cruise surveyed the southern part of EJS from June 17^{th} to July 21^{st}, and the second one covered the northern part of EJS from July 22^{nd} to August 11^{th} 1999. Detailed information on the cruises is described in Talley *et al.* (2004), and the hydrographic datasets are available at http://sam.ucsd.edu/onr_data/. Recently, Kim and Lee (2004) defined the physicochemical characteristics of eight different water masses involved in the EJS's circulation and estimated their mixing ratios by applying the Optimum Multiparameter (OMP) method to the high-resolution CREAMS II data. Here, we use the mixing ratio of ESIW estimated by Kim and Lee (2004), and temperature, salinity, pressure, DO, phosphate, and pCFC12 age data for the isopycnic analysis of ESIW. The pCFC12 age is a water mass ventilation time scale derived from CFC measurement in the ocean.

Kim and Lee (2004) considered both geographical locations and properties of temperature, salinity, and DO to define the characteristics of eight water masses (Fig. 2): (1) North Korea Surface Water (NKSW) is the surface waters near 41°N with higher temperature and lower salinity ($T \geq 20°C$ and $S \leq 33$ psu). It represents low salinity surface waters in the northern EJS (Fig. 2a); (2) East Korean Coastal Water (EKCW) is defined as the warm and less saline waters ($T \geq 20°C$ and $33° \; S < 34$ psu) at surface distributing along the coast of western EJS from the Korea Strait (KS) (Fig. 2b). It is one of the branches of Tsushima Warm Current (TWC) (Lee and Chung, 1981); (3) Modified Tsushima Surface Water (MTSW) for the warm and saline surface waters ($T \geq 20°C$ and $S \geq 34$ psu) that are widely distributed from the eastern channel of the KS to the subpolar front at ~40°N (Fig. 2c). Park (1978) and Yang *et al.* (1991) defined the surface waters showing $T > 20°C$ and $S < 33.8$ psu as Tsushima Surface Water (TSW). But because of its high salinity feature (> 34 psu), this water mass is called MTSW; (4) Tatar Surface Cold Water (TSCW) for the surface waters with low temperature and salinity ($T \leq 20°C$ and $S \leq$

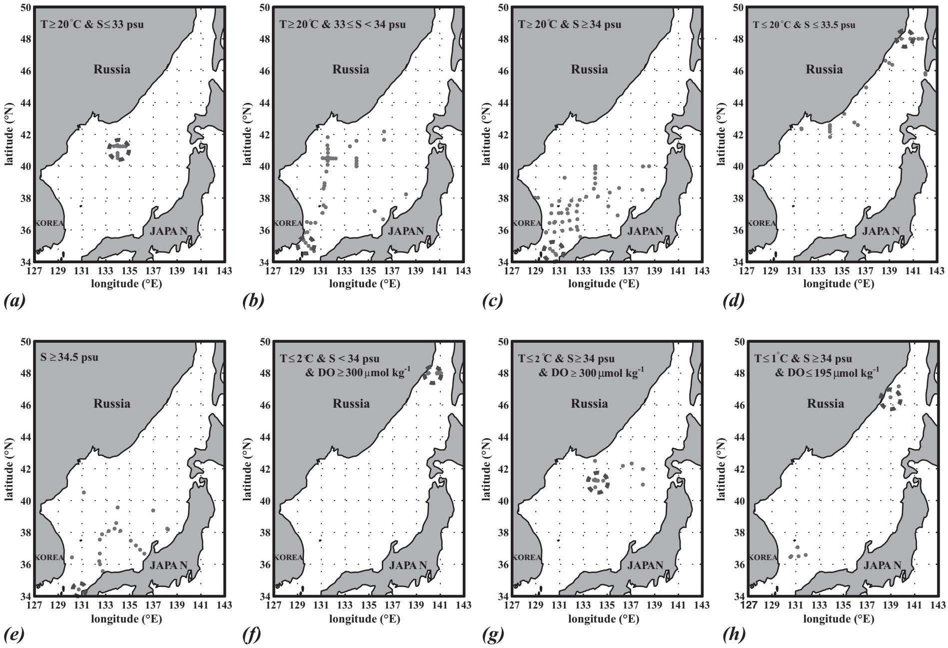

Figure 2. Hydrographic stations (dots) satisfying the conditions to be individual source water type and focal regions (dotted circle) to define the physicochemical characteristics of source water types (adopted from Fig. 2 of Kim and Lee, 2004). Eight different source water types are defined for the OMP analysis. (a) North Korea Surface Water (NKSW), (b) East Korean Coastal Water (EKCW), (c) Modified Tsushima Surface Water (MTSW), (d) Tatar Surface Cold Water (TSCW), (e) Tsushima Middle Water (TMW), (f) Liman Cold Water (LCW), (g) East Sea Intermediate Water (ESIW), and (h) East Sea Proper Water (ESPW).

33.5 psu) along the Russian coast from the Tatar Strait (TtS) (Fig. 2d); (5) Tsushima Middle Water (TMW) for the high salinity waters along the coast of Japan from the KS ($S \geq 34.5$ psu), (Lim and Chang, 1969; Park, 1978; Kim and Kim, 1983; Yang *et al.,* 1991) (Fig. 2e). These waters are the main stream of TWC (Kawabe, 1982; Yoon, 1982; Hong and Cho, 1983); (6) Liman Cold Water (LCW) for the low temperature (≤ 2°C), low salinity (< 34 psu), and high DO (≥ 300 μmol kg^{-1}) waters in the TtS (Fig. 2f); (7) East Sea Intermediate Water (ESIW) for the waters of $1°C < T < 3°C$, $S \geq 34$ psu, and DO $\geq$ 300 μmol kg^{-1} as defined by Kim and Chung (1984) (Fig. 2g); (8) East Sea Proper Water (ESPW) for the deep waters with $T \leq 1°C$, $S \geq 34$ psu, and DO ≤ 195 μmol kg^{-1} as defined by Uda (1934), Lim and Chang (1969), and Kim *et al.* (1996) (Fig. 2h). The characteristics of the eight different source water types used in the OMP analysis in Kim and Lee (2004) are summarized in Table 1, and their temperature and salinity characteristics are identified on T-S diagram (Fig. 3).

The OMP analysis is an inverse method based on an over-determined linear system. The basic structure of OMP analysis is written as:

Table 1. The characteristics of eight source water types (SWT) defined for OMP analysis in the East/Japan Sea (adopted from Table 2 of Kim and Lee, 2004).

SWT	T (°C)	S (psu)	DO (μmol kg^{-1})	Si (μmol kg^{-1})	NO_3 (μmol kg^{-1})	PO_4 (μmol kg^{-1})	T. Alk.* (μmol kg^{-1})	pH
NKSW	23.697	32.658	217.9	3.20	0.14	0.02	2177.3	8.00
EKCW	21.381	33.706	226.8	3.30	0.05	0.07	2248.3	8.08
MTSW	22.464	34.220	222.6	1.90	0.04	0.04	2262.0	8.07
TSCW	13.620	32.750	266.8	2.20	0.02	0.06	2210.4	7.91
TMW	19.528	34.504	219.1	2.90	0.85	0.17	2281.6	8.02
LCW	1.742	33.829	351.4	6.20	3.61	0.45	2262.6	7.80
ESIW	1.436	34.042	318.5	16.80	11.44	0.91	2264.5	7.68
ESPW	0.175	34.065	197.6	89.40	25.86	2.12	2284.6	7.39

*T. Alk.: Total Alkalinity.

$$G \cdot x - d = R \tag{1}$$

where G is the physicochemical characteristics of source water types defined (e.g. Table 1) and is given as matrix form, x is the mixing ratios of source water types and is represented

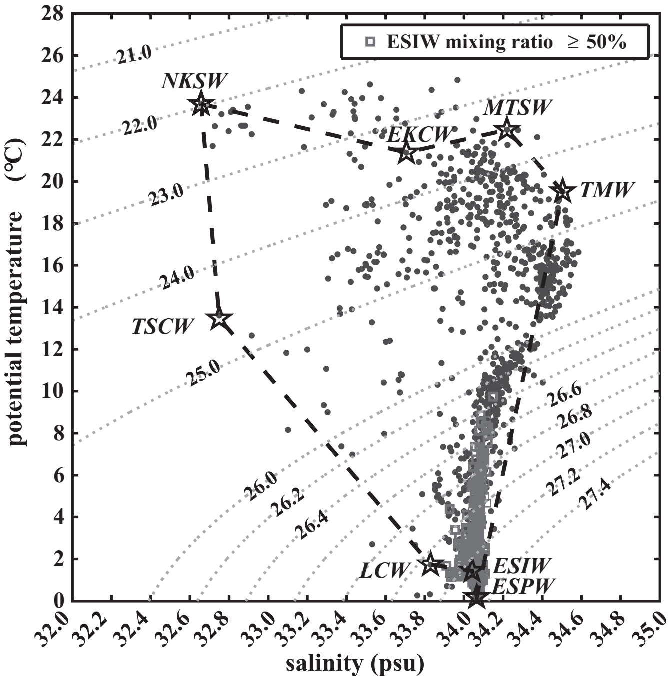

Figure 3. Temperature and salinity characteristics of source water types used in the OMP analysis by Kim and Lee (2004). The square symbols indicate the data of mixing ratios of pure ESIW greater than 50%. EKCW, TSCW, NKSW, MTSW, TMW, LCW, source water of ESIW, and ESPW are also marked on T-S diagram.

Table 2. The potential density (σ_θ) range and core layer of ESIW defined in the East/Japan Sea. The estimate by current study is for the pure ESIW mixing ratios greater than 50%.

Density layer σ_θ (kg m^{-3})	Core surface or layer σ_θ (kg m^{-3})	Observation season	Ref.
26.90–27.30	27.20	Summer 1995	Kim and Kim (1999)
26.90–27.30	27.20	Summer 1993–96	Kim *et al.* (2004)
27.00–27.32	27.28	Summer and fall 1969	Senjyu (1999)
ND	27.10–27.20	Summer 1999	Talley *et al.* (2006)
27.14–27.26	27.221	Summer 2005	Shin (2006)
26.90–27.30	27.20	1963–1993	Shin *et al.* (2007)†
26.30–27.34	**27.20–27.30**	**Summer 1999**	**This study (2010)**

ND: not defined.

†Shin *et al.* (2007) use the historical data obtained from Maizuru Marine Observatory (MMO) for 1963–1992 and from Korean Ocean Research and Development Institute (KORDI) for 1990–1993.

as column vector, d is composed of physicochemical observations and is given as column vector, and R is the column vector of residuals. The OMP analysis finds the mixing ratio x by minimizing R with the constraints of mass conservation and non-negative solution:

$$\sum_{i=1}^{n} x_i = 1 \qquad (x_i \geq 0). \tag{2}$$

Detailed information about the OMP analysis method is described in Tomczak and Large (1989). Temperature, salinity, dissolved oxygen, total alkalinity, pH, silicate, nitrate, and phosphate are used for the OMP analysis (Table 1), and the typical range of residuals for ESIW mixing ratio is within 2% (Kim and Lee, 2004). ESIW is mainly mixing with ESPW and LCW (Fig. 5a). We refer to ESIW for both source and subducted waters in this work because our analysis is based on the mixing ratio of ESIW estimated by the OMP analysis.

3. Results

a. Physicochemical properties of the ESIW core density layer

i. The core density layer of the ESIW based on its mixing ratios. Water masses can move efficiently along the same density layer (i.e. isopycnal), so the isopycnic analysis can better depict the physicochemical properties of a spreading water mass than the conventional depth-based analysis. The potential density of ESIW ranges from 26.90 to 27.32, and typically defined at 27.2 according to previous results (Kim and Kim, 1999; Senjyu, 1999; Kim *et al.,* 2004; Shin, 2006; Talley *et al.,* 2006; Shin *et al.,* 2007), which are summarized in Table 2. However, the core density layer of ESIW has not been defined clearly. Here, we present the potential density range of ESIW and define its core density layer, in terms of its water mass mixing ratio, for summer 1999.

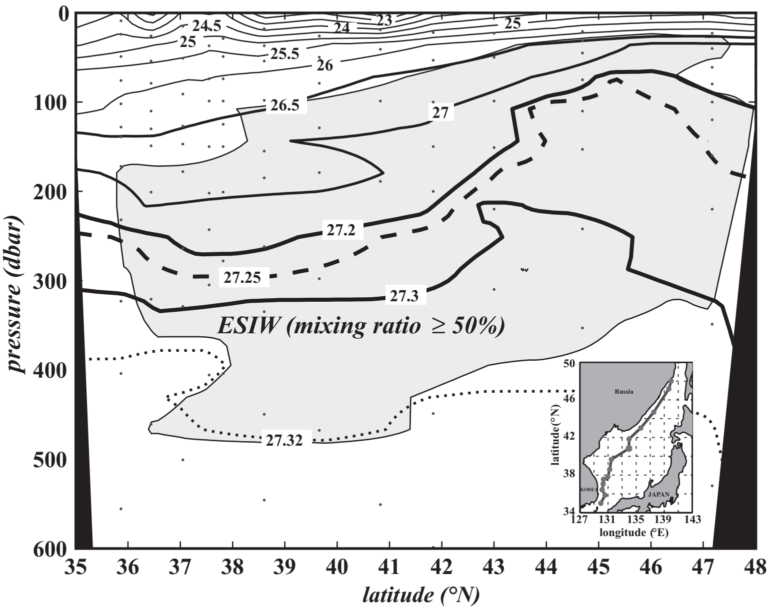

Figure 4. Meridional distribution of potential density, σ_θ, for the upper 600 dbar layer in EJS in summer 1999. The gray shade area represents the distribution of waters with pure ESIW mixing ratio greater than 50%. The locations of stations are shown in the insert map.

The spatial distribution of potential density in EJS is described along a meridional section in Figure 4. The gray area corresponds to waters with ESIW mixing ratio greater than 50% which is distributed between σ_θ = 26.50 and 27.32. This range is consistent with those reported from previous studies (σ_θ = 26.90–27.32). However, the core density layer of ESIW is difficult to define from the spatial distribution of density alone. Thus, we plot the ESIW mixing ratio versus the potential density to delineate waters of ESIW mixing ratio greater than 50% (Fig. 5). Density of the higher ESIW mixing ratio (≥ 50%) ranges from 26.329 to 27.334 (Fig. 5a). Within this range, the potential density between 27.2 and 27.3 exhibits the highest mixing ratio and concentrated data distribution (Fig. 5b). As a result, we define the core density layer of ESIW for 1999 to σ_θ = 27.2–27.3 within its broader density range of σ_θ = 26.329–27.334. Hereafter, we present the physicochemical properties of ESIW at the core layers of σ_θ = 27.20, 27.25, and 27.30 surfaces.

ii. Physical property and mixing ratio distributions. The deeper part of EJS is separated by three major basins: JB, UB, and YB (Fig. 1). To facilitate the presentation of our analysis, we divide JB into WJB and EJB along 135°E (Fig. 6). On σ_θ = 27.20 and 27.25 surfaces, the water with the ESIW mixing ratio greater than 75% is widely distributed in JB except for the eastern boundary, and the mixing ratio decreases to the south (Figs. 6a, b). The spatial extent of the ESIW mixing ratio is greater than 75% on the σ_θ = 27.30 surface

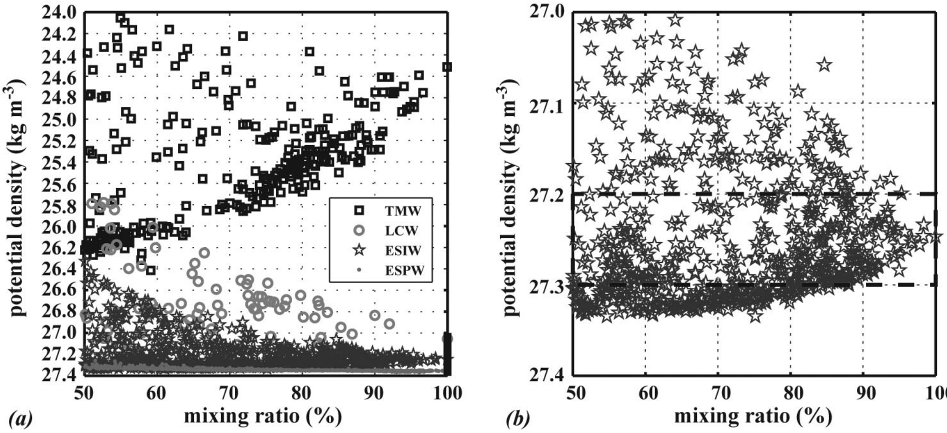

Figure 5. (a) Mixing ratios (≥ 50%) versus potential density of TMW, LCW, ESIW, and ESPW. (b) Zoom in version of (a) for the result of ESIW mixing ratios vs. potential density between σ_θ = 27.0 and 27.4. Higher ESIW mixing ratios are concentrated between σ_θ = 27.2 and 27.3. We define σ_θ = 27.2–27.3 as core density layer of ESIW.

shrinks compared to those on σ_θ = 27.20 and 27.25 surfaces (Fig. 6c). Overall, the ESIW mixing ratio is higher in JB than in UB and YB on these density surfaces.

The depth distributions of σ_θ = 27.20 and 27.25 surfaces show that these layers are shallower than 100 dbar and distributed widely in JB, and the layers become deeper near the subpolar front (~40°N) toward UB (Figs. 6d, e). These layers shoal to less than 100 dbar near the Korean coast in UB (Figs. 6d, e). The σ_θ = 27.30 surface clearly deepens steeply at the subpolar front to UB (Fig. 6f). Such a feature is also shown at the edges of EJB (Fig. 6f). The depth structure of the ESIW seems to dome up in JB, deepen at the subpolar front (~40°N), and bowl down in UB and YB.

The isopycnic ESIW distributions from this study (Fig. 6) are complementary to vertical distributions of ESIW estimated on depth space previously (Kim and Lee, 2004; see their Figs. 5c, g), as they are based on the same OMP analysis technique and datasets. Despite differences in end member settings, the ESIW distribution described previously (Kim and Lee, 2004; Min and Warner, 2005) are compatible in terms of lateral and vertical distributions of higher ESIW mixing ratios. The composition of ESIW layer was explained with 8 source waters (Kim and Lee, 2004), and four of them (ESIW, TMW: Tsushima Middle Water, LCW: Liman Cold Water, and ESPW: East Sea Proper Water) playing the major role in mixing (Fig. 5a). ESIW and LCW are fresher types, TMW is a warmer and saline type, and ESPW is a deeper component of mixing in the layer. On the other hand, Min and Warner (2005, see their Figs. 19–21) used only three source waters which were characterized by different parameter choices including CFC tracers observed in 1999: (i) low salinity water in JB, (ii) Tsushima Warm Water, and (iii) Central Water, and they were analogous to ESIW and LCW, TMW, and ESPW source water types, respectively,

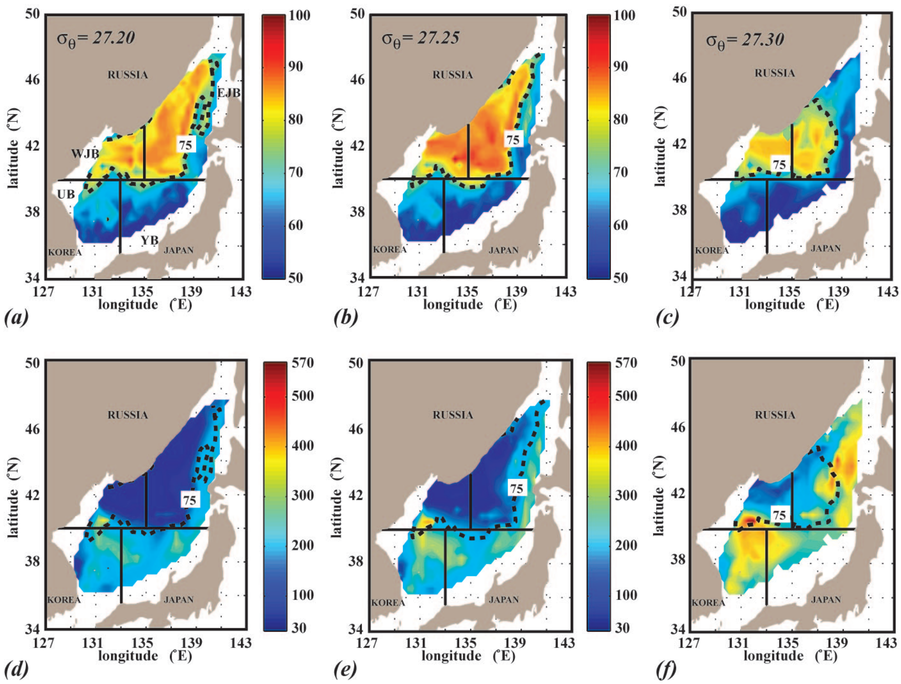

Figure 6. Horizontal distributions of physical mixing ratio and pressure of ESIW at its core layer (σ_θ = 27.20–27.30). (a)–(c) ESIW mixing ratio (%) on σ_θ = 27.20, 27.25, and 27.30, respectively, (d)–(f) pressure of ESIW layer (dbar) of the corresponding surfaces in (a)–(c). Solid lines are the boundary to distinguish each basin, and W/EJB stands for western/eastern Japan Basin. The black dashed line is a contour line delineates the 75% ESIW mixing ratio as a reference.

described before (Kim and Lee, 2004). Due to different end member choices, these ESIW mixing ratios (Kim and Lee, 2004; Min and Warner, 2005) were slightly different in the northern JB, but overall these two estimates were compatible.

iii. Biogeochemical properties distributions. The spatial distributions of biogeochemical properties such as DO and phosphate on σ_θ = 27.20, 27.25, and 27.30 surfaces are noteworthy. The highest DO concentration ($\geq$ 330 μmol kg^{-1}) occurred off the Primorye coast in WJB (Fig. 7a). The high DO-content area in JB ($\geq$ 280 μmol kg^{-1}) was distinguished from the low DO-content regions in UB and YB (< 280 μmol kg^{-1}) across the subpolar front (Figs. 7a, b). The oxygen distribution pattern was similar in the σ_θ = 27.3 layer (Fig. 7c). A lower oxygen-content water throughout three density layers was evident along the Japanese coast in EJB, indicating that the ESIW was losing its originality and mixing with ESPW (Fig. 5a). The distribution of dissolved oxygen was similar to that of the mixing ratio.

The distribution of phosphate was nearly opposite to that of dissolved oxygen (Figs. 7e–f). The concentration of phosphate was low in the JB and high in UB and YB. The

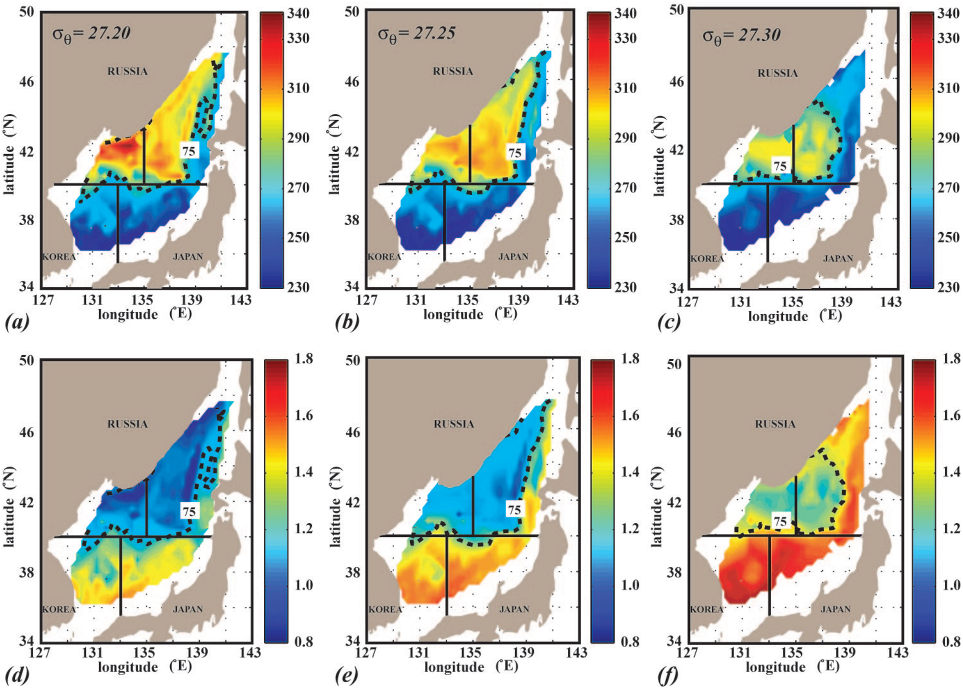

Figure 7. Horizontal distributions of the biogeochemical properties of ESIW in its core density layer (σ_θ = 27.20–27.30). (a)–(c) dissolved oxygen (μmol kg^{-1}) on σ_θ = 27.20, 27.25, and 27.30, respectively, (d)–(f) phosphate (μmol kg^{-1}) on the corresponding surfaces as (a)–(c).

distributions of DO and nutrients have been used widely to identify the passage of water masses indirectly (Broecker and Peng, 1982; Broecker, 1991). Based on the distributions of DO and phosphate, we conclude that the ESIW originates in WJB, and the ESIW is younger in JB than in UB and YB. Also, the chemical properties show a large north-south gradient across the subpolar front. The ranges of physicochemical property values of ESIW at the core layer are summarized in Table 3.

Table 3. The upper and lower boundaries of physicochemical properties of waters with pure ESIW mixing ratios greater than 50% ($27.2 \leq \sigma_\theta \leq 27.3$).

Pressure (dbar)	DO (μmol kg^{-1})	Phosphate (μmol kg^{-1})	Nitrate* (μmol kg^{-1})	Silicate* (μmol kg^{-1})
32 – 568	233.08 – 340.58	0.82 – 1.76	10.49 – 22.66	15.33 – 39.02

*Distributions of nitrate and silicate are not shown in figures because their spatial patterns are similar to that of phosphate distribution.

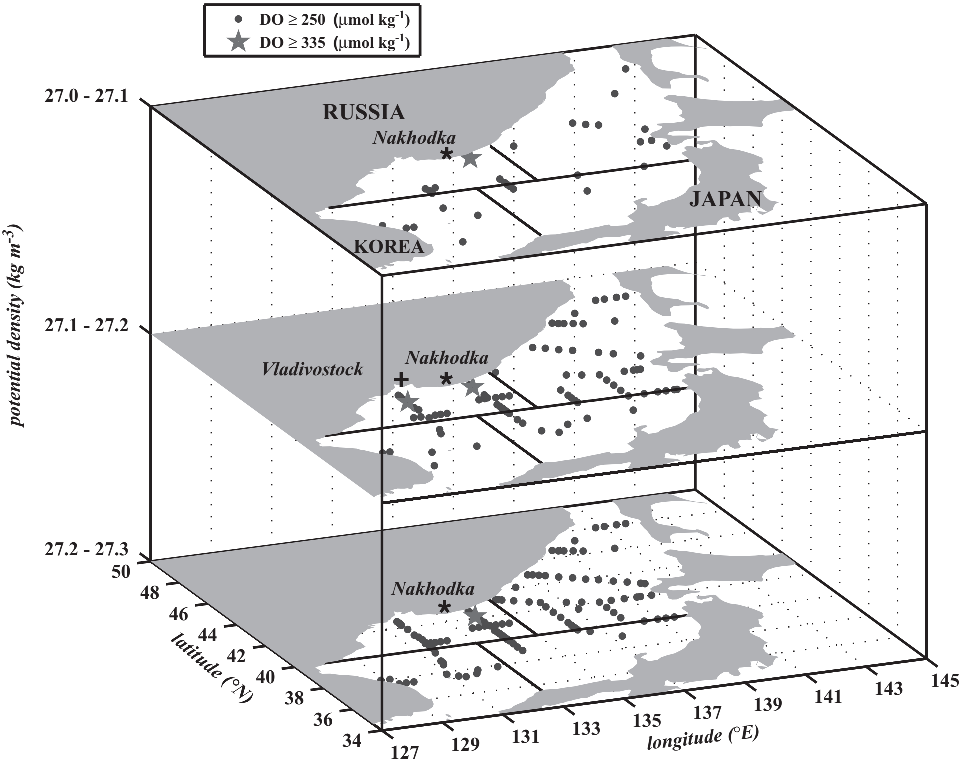

Figure 8. Spatial distribution of the hydrographic stations with high dissolved oxygen of ESIW ($\geq$ 250 μmol kg^{-1}) in the isopycnic layers of σ_θ = 27.0–27.1, 27.1–27.2, and 27.2–27.3. The star symbols indicate the stations showing oxygen concentration greater than 335 μmol kg^{-1}.

b. Locations of formation and subduction of ESIW inferred from oxygen distribution

DO and AOU are used to infer the location of formation and ventilation of ESIW. The hydrographic stations with DO $\geq$ 250 μmol kg^{-1} are mapped on the isopycnal surfaces to infer the ESIW formation areas (Fig. 8). This DO criterion is also used to characterize ESIW elsewhere (Kim and Kim, 1999; Yoon and Kawamura, 2002; Kim *et al.,* 2004). They are distributed rather broadly in JB, so the formation region of ESIW is difficult to pinpoint with this threshold value. The hydrographic stations with the highest DO concentration ($\geq$335 μmol kg^{-1}) are depicted by the star symbol in Figure 8. Those with DO $\geq$ 335 μmol kg^{-1} are confined to the Russian Primorye coast (Vladivostok-Nakhodka). This result is consistent with previous studies (Seung, 1997; Kim and Kim, 1999; Yoon and Kawamura, 2002; Kim *et al.,* 2004) reporting that the ESIW is formed near the Russian coast in WJB. This implies that the EJS's THC begins off the Primorye coast.

We present the spatial distribution of AOU with the pressure surface to scrutinize the subduction and ventilation processes of ESIW on σ_θ = 27.20, 27.25, and 27.30 surfaces

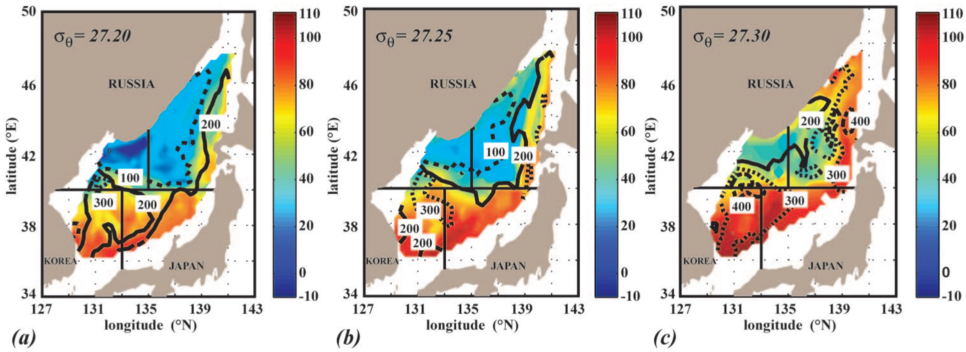

Figure 9. Horizontal distribution of AOU (μmol kg^{-1}) on σ_θ = (a) 27.20, (b) 27.25, and (c) 27.30 surface, respectively. The color maps show the spatial distribution of AOU, and the black contour lines represent the pressure (dbar) of the corresponding density surfaces.

(Fig. 9). The lowest concentration of AOU (≤ 0 μmol kg^{-1} or super-saturated) were found in WJB (Fig. 9a). A slightly higher value close to the atmospheric equilibrium value of AOU observed in EJB (Figs. 9a, b) will be discussed in detail later. The low AOU extending to the Tatar Strait (TtS) may relate to Liman Cold Water (LCW), which originates in TtS and has higher DO concentrations similar to ESIW (Fig. 5a and Table 1). Low AOU concentrations (≤ 50 μmol kg^{-1}) were distributed widely in JB along the 200 dbar contour, whereas UB and YB had higher AOU concentrations (> 50 μmol kg^{-1}) (Fig. 9b). The σ_θ = 27.30 surface showed a similar AOU distribution contrasting JB vs. UB and YB (Fig. 9c). All three isopycnal surfaces steeply deepened to the south at 131–133°E and 40–41°N, indicating subduction of ESIW at this area (Senjyu, 1999; Yoshikawa *et al.,* 1999; Shin, 2006). The distributions of AOU and pressure suggest that the ESIW was formed in WJB, with one branch spreading to EJB and the other branch intruding southward into UB via subduction at 131–133°E across the subpolar front.

Some pressure surfaces shoaled near the Korean coast in UB (Fig. 9), and were observed frequently as coastal upwelling (Lee, 1983; Lee and Na, 1985). More information is needed to explain whether the ESIW subducted near the subpolar front was uplifted, or if a different branch of the ESIW flowed south along the east coast of Korea (Kim and Kim, 1983; Shin, 2006). Unfortunately, the data for the North Korean waters, to identify the branch of ESIW flowing south along the coast, is not available. Nevertheless, the observation implies that the coastal upwelling in the southwestern EJS may be influenced by the subduction of ESIW at the subpolar front between UB and WJB (Lee and Kim, 2003).

4. Discussion

a. *Estimation of the relative age of ESIW*

A so-called "pseudo-age" (referred to here as "relative age") concept, designed to estimate water mass age from the relationship of AOU to oxygen utilization rate (OUR)

Table 4. The oxygen utilization rate (OUR) in the East/Japan Sea expressed as the function of depth (z).

Depth range (m)	OUR (z) (μmol·kg^{-1} · yr^{-1})	Basin	Tracer age used	Ref.
200–1600	$29 \times e^{-0.00095 \times Z}$	WJB	^{3}H-^{3}He	Hahm and Kim (2008)
200–1000	$5 \times e^{-0.001573 \times Z}$	EJB, UB, YB	Mean mixing age (CFCs-based model)	Min (1999)

(Poole and Tomczak, 1999), was applied to estimating the ventilation age of the ESIW. AOU is estimated as:

$$\mathrm{AOU} = [O_2^{sat}] - [O_2^{obs}] \tag{3}$$

where $[O_2^{sat}]$ is the saturated oxygen concentration theoretically calculated by solubility as a function of temperature and salinity (Weiss, 1970) and $[O_2^{obs}]$ is the observed DO concentration.

Low surface water oxygen saturation (< 82% and 92%) was observed in WJB during winter 2001 (Talley *et al.,* 2003). This wintertime surface water oxygen disequilibrium occurs when the outbreak of cold air from the Siberia causes dense surface waters to mix deep without having enough time to equilibrate with the atmosphere. OUR was estimated in WJB as a function of depth (200–1600 m) with the tritium-helium (^{3}H-^{3}He) age data for various the initial oxygen saturations (i.e., 80%, 90%, and 100%) (Hahm and Kim, 2008). An OUR value covering the whole water column of EJS was suggested from the mean mixing age estimated by a steady state box model calibrated by CFCs tracer data (Min, 1999). The OUR value of Hahm and Kim (2008) is applied to WJB, and another OUR value of Min (1999) is used for the rest of the basins, EJB, UB, and YB, to estimate the relative age of ESIW (Table 4). For example, the OUR at 500 m depth in WJB and EJB would be 18.0 and 2.3 μmol kg^{-1} yr^{-1}, respectively. We estimate the relative age of ESIW according to the surface water oxygen saturation conditions of 80%, 90%, and 100%. The relative age can be computed as:

$$relative\ age\ (year) = \frac{[O_2^{sat}]_{80,90,100\%} - [O_2^{obs}]}{\mathrm{OUR}} = \frac{\mathrm{AOU}_{80,90,100\%}}{\mathrm{OUR}} \tag{4}$$

where the unit of AOU is μmol kg^{-1}, and that of OUR is μmol kg^{-1} yr^{-1}. We estimate the relative age below 200 m depth, and use the pCFC12 age data to diagnose the previous wintertime oxygen saturation condition at the surface.

As shown in Figure 10a, the maximum relative age of ESIW according to the oxygen saturation levels of 80%, 90%, and 100% is approximately 11, 23, and 36 years, respectively, and the pCFC12 age ranges from 10 to 18 years. We use the correlation coefficient (R) between the pCFC12 and relative age estimated at oxygen saturation 80%, 90%, and 100% to infer the current oxygen saturation condition at the surface of EJS (Fig.

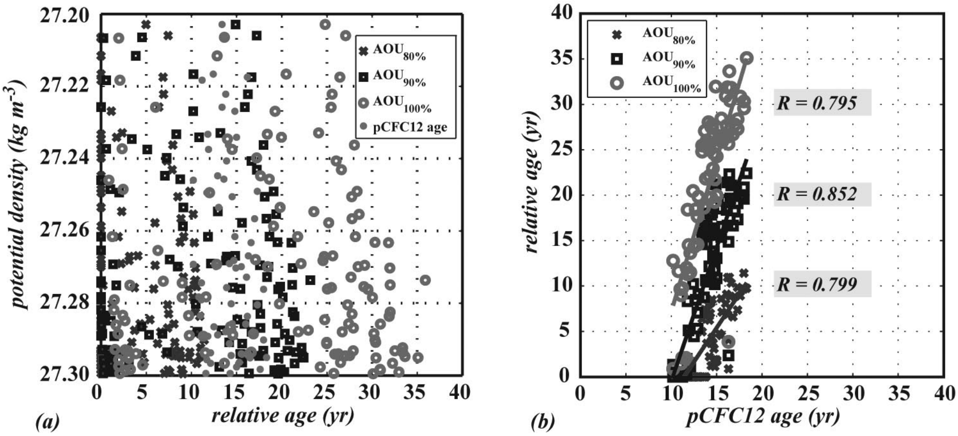

Figure 10. Distributions of the relative and pCFC12 ages of ESIW (mixing ratio ≥ 50%) within its core density layer (σ_θ = 27.2–27.3). The relative age is estimated at the surface oxygen saturation conditions of 80%, 90%, and 100%. The negative values for super-saturated condition are displaced to zero. (a) Relative age *vs.* potential density, (b) pCFC12 age *vs.* relative age estimated at surface water oxygen saturation condition of 80%, 90%, and 100%.

10b). The result from the relationship between the pCFC12 and relative age with the initial oxygen saturation of 90% has the highest correlation coefficient (0.852), suggesting that the wintertime disequilibrium condition of oxygen at the surface of EJS is about 90%. The maximum relative age or ventilation time of 23.3 years at oxygen saturation of 90% corresponds well with 20.3–25.6 years of time scale estimated by Yoshikawa *et al.* (1999).

ESIW participates in the shallow- to mid-depth THC in EJS with decadal-scale ventilation time. Recently, the increase in the winter air and sea surface temperatures in EJS region was speculated to be caused by global warming (Gamo, 1999; Min and Kim, 2006). Such changes may exacerbate the disequilibrium of oxygen at the surface and disturb the formation of the ESIW. Eventually, the EJS's THC might be substantially weakened, and this issue warrants more continuous observations of ESIW in the EJS.

b. Co-existence of high- and low-salinity intermediate waters in JB

The relatively low AOU feature in EJB, in contrast to that in WJB (Figs. 9a, b), is examined further. The horizontal distribution of $AOU_{90\%}$ on $\sigma_\theta = 27.25$ surface overlaid by the salinity contour map along with the relative and pCFC12 ages is presented in Figure 11. Note that the pCFC12 age distribution is overlaid with the potential temperature contour map (Fig. 11c), and all the distributions in Figure 11 are below a depth of 200 m. The shape of the AOU distribution in JB is quite symmetrical (Fig. 11a), i.e. there are two source regions showing the lowest AOU, and AOU increases away from each core region. Such distributions appear in the relative and pCFC12 age maps as well showing young waters in WJB and EJB (Figs. 11b, c). They imply that the source region shown in EJB is

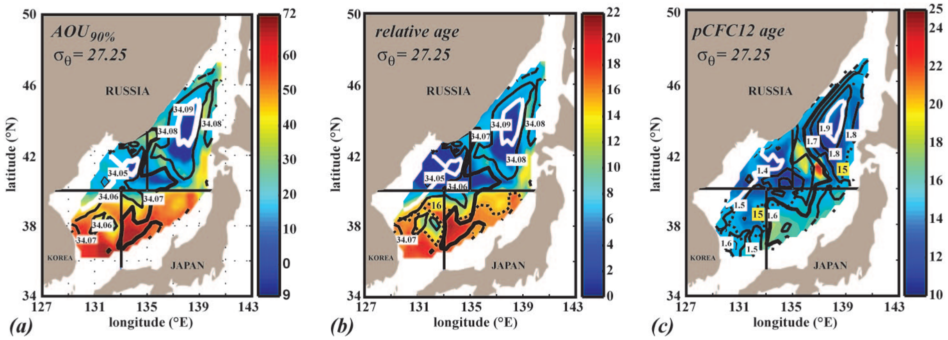

Figure 11. Spatial distributions of (a) AOU (μmol kg^{-1}) at surface water oxygen saturation condition of 90%, (b) relative age (yr), and (c) pCFC12 age (yr) of the ESIW on $\sigma_\theta = 27.25$ surface. The salinity (psu) distributions are overlaid on (a)–(b) as contour lines, and that of potential temperature (°C) on (c). Only the data from below the depth of 200 m depth are analyzed. A dotted contour line indicates 15 (16) years of pCFC12 (relative ages).

another location of intermediate water formation, with higher salinity (~34.1 psu) and temperature (~2°C) characteristics.

High salinity water with high oxygen content was observed in EJB and labeled High-Salinity Intermediate Water (HSIW) (Kim and Kim, 1999). The HSIW has typical values of potential temperature, salinity, DO, and potential density ranges of 1–5°C, $S > 34.07$ psu, DO > 250 μmol l^{-1}, and 27.0–27.32 σ_θ, respectively (Kim and Kim, 1999; Kim *et al.,* 2004). Except for salinity, other characteristics are identical with the ESIW's. AOU can be another useful criterion to distinguish the ESIW and HSIW (Fig. 11a; Shin *et al.,* 2007). The distributions of relative and pCFC12 ages show the circulation patterns of two intermediate waters (Figs. 11b, c). A dotted contour line of 15 (16) years of pCFC12 (relative ages) extends farther into UB, suggesting that one branch of ESIW moves into UB. The relative and pCFC12 ages are relatively high at the center of EJS. These characteristics result from the mixing between ESIW and HSIW by cyclonic circulation in JB; the ESIW flows to the east, whereas the HSIW flows to the west (Isobe and Isoda, 1997; Seung, 1997; Kim and Kim, 1999; Kim and Seung, 1999).

In the meantime, the distributions of relative and pCFC12 ages along with salinity and potential temperature in UB and YB suggest a possibility that other branch of HSIW intrudes into YB. The YB is occupied by a high salinity (> 34.07 psu), high potential temperature (> 1.6°C), and old age (relative age > 13 years; pCFC12 age > 15 years) waters originating in EJB. These characteristics are distinguishable from the UB. The process of HSIW flowing into YB is slower than the ESIW's spreading to UB, preventing it from recognition in previous studies. The salinity and potential temperature of ESIW were lower than those of HSIW. Thus, cooling is a key factor to forming ESIW, whereas the supply of salt is more important for HSIW (Watanabe *et al.,* 2001). The ESIW and HSIW circulate cyclonically in JB, and each branch flows to the UB and YB, respectively.

5. Summary

Recent studies on EJS reported changes in DO in intermediate and deep waters due to impacts on THC by climate change and global warming. The ESIW plays an important role in supplying DO and transporting anthropogenic carbon into the intermediate/deep layers of EJS. The study of the ESIW formation and distribution processes may provide insights on the THC of EJS and its response to climate forcing. The current study analyzes the core density layer, physicochemical properties and their spatial distributions, and potential locations of formation and subduction of ESIW and its interaction with HSIW. The core density layer of ESIW is defined at $\sigma_\theta = 27.2$–27.3, based on the higher mixing ratio of pure ESIW. The DO and mixing ratio of ESIW are higher in JB than in UB and YB, and the pressure structure is domed in JB then steeply deepens southward underneath the subpolar front (~40°N) where it is bowled in UB and YB. The distribution of phosphate is grossly opposite to that of dissolved oxygen. The hydrographic stations with high DO (≥ 250 μmol kg^{-1}), characteristic of ESIW, are broadly distributed in JB, and those with the highest DO concentrations (≥ 335 μmol kg^{-1}) are limited to the Primorye coast, indicating the potential formation site of the ESIW. The subduction of ESIW into UB occurs at 131–133°E and 40–41°N. Noticeably, some pressure surfaces rise near the Korean coast in UB, implying a link between coastal upwelling and ESIW subduction in the southwestern EJS. The maximum relative age of ESIW at 90% oxygen saturation is about 23 years, and the pCFC12 age is 10–18 years. The good correlation between the pCFC12 and relative age at 90% of the initial surface water oxygen saturation suggests that this might be a wintertime disequilibrium condition at the surface of EJS. ESIW coexists with HSIW at the same density layer in some areas, and these two intermediate waters circulate cyclonically in JB. Each branch of them flows to UB and YB. Our analysis suggests that ESIW is sensitive to climate forcing and an important shallow-to-mid depth THC component of EJS.

Acknowledgments. We wish to thank all the people who contributed to the CREAMS II program. We thank F. Primeau (University of California Irvine) for invaluable discussions concerning an earlier draft and C. Grall (University of Miami) and W. Gardner (University of Texas at Austin) for reading the manuscript and making valuable suggestions. Tongsup Lee is generously supported by EAST-1 program. This is the University of Texas, Marine Science Institute's contribution number 1605.

REFERENCES

Broecker, W. S. 1991. The great ocean conveyor. Oceanogr., *4,* 79–89.

Broecker, W. S. and T.-H. Peng. 1982. Tracers in the Sea, Eldigio Press, Palisades, NY, 690 pp.

Chae, Y. K., Y. H. Seung and S. K. Kang. 2005. Mode change of deep water formation deduced from slow variation of thermal structure: One-dimensional model study. Ocean Polar Res., *27,* 115–123.

Chen, C. T. A., A. S. Bychkov, S. L. Wang and G. Yu. Pavlova. 1999. An anoxic Sea of Japan by the year 2200? Mar. Chem., *67,* 249–265.

Gamo, T. 1999. Global warming may have slowed down the deep conveyor belt of a marginal sea of the northwestern Pacific: Japan Sea. Geophys. Res. Lett., *26,* 3137–3140.

Hahm, D. and K.-R. Kim. 2008. Observation of bottom water renewal and export production in the Japan Basin, East Sea using tritium and helium isotopes. Ocean Sci. J., *43,* 39–48.

Hong, C. H. and K. D. Cho. 1983. The northern boundary of the Tsushima Current and its fluctuations. J. Korean Soc. Oceanogr., *18,* 1–9.

Isobe, A. and Y. Isoda. 1997. Circulation in the Japan Basin, the northern part of the Japan Sea. J. Oceanogr., *53,* 373–381.

Kang, D.-J., J.-Y. Kim, T. Lee and K. R. Kim. 2004. Will the East/Japan Sea become an anoxic sea in the next century? Mar. Chem., *91,* 77–84.

Kang, D.-J., K.-E. Lee and K.-R. Kim. 2003. Recent development in chemical oceanography of the East (Japan) Sea with an emphasis on CREAMS finding: A review. Geosci. J., *7,* 179–197.

Kawabe, M. 1982. Branching of the Tsushima Current in the Japan Sea Part II. Numerical experiment. J. Oceanogr. Soc. Japan, *38,* 183–192.

Kim, C. H. and K. Kim. 1983. Characteristics and origin of the cold water mass along in the east coast of Korea. J. Korean Soc. Oceanogr., *18,* 73–83.

Kim, I.-N. and T. Lee. 2004. Summer hydrographic features of the East Sea analyzed by the Optimum Multiparameter method. Ocean Polar Res., *26,* 581–594.

Kim, K., K.-I. Chang, D.-J. Kang, Y. H. Kim and J.-H. Lee. 2008. Review of recent findings on the water masses and circulation in the East Sea (Sea of Japan). J. Oceanogr., *64,* 721–735.

Kim, K and J. Y. Chung. 1984. On the salinity minimum and dissolved oxygen maximum layer in the East Sea (Sea of Japan), *in* Ocean Hydrodynamics of the Japan and East China Seas, T. Ichiye, ed., Elsevier, 55–65.

Kim, K., K.-R. Kim, J. Y. Chung, H. S. Yoo and S. G. Park. 1991. Characteristics of physical properties in the Ulleung Basin. J. Korean Soc. Oceanogr., *26,* 83–100.

Kim, K., K.-R. Kim, Y. G. Kim, Y. K. Cho, J. Y. Chung, B. H. Choi, S. K. Byun, G. H. Hong, M. Takematsu, J. H. Yoon, Y. Volkov and M. Danchenkov. 1996. New findings from CREAMS observation: Water masses and eddies in the East Sea. J. Korean Soc. Oceanogr., *31,* 155–163.

Kim, K., K.-R. Kim, Y. G. Kim, Y. K. Cho, D.-J. Kang, M. Takematsu and Y. Volkov. 2004. Water mass and decadal variability in the East Sea (Sea of Japan). Prog. Oceanogr., *61,* 157–174.

Kim, K., K.-R. Kim, D.-H. Min, Y. Volkov, J.-H. Yoon and M. Takematsu. 2001. Warming and Structural changes in the East Sea(Japan Sea): A clue to future changes in global oceans? Geophys. Res. Lett., *28,* 3293–3296.

Kim, K. J. and Y. H. Seung. 1999. Formation and movement of the ESIW as modeled by MICOM. J. Oceanogr., *55,* 369–382.

Kim, K.-R. and K. Kim. 1996. What is happening in the East Sea (Japan Sea)? Recent chemical observations during CREAMS 93–96. J. Korean Soc. Oceanogr., *31,* 164–172.

Kim, K.-R., G. Kim, K. Kim, V. Lobanov, V. Ponomarev and A. Salyuk. 2002. A sudden bottom-water formation during the severe winter 2000–2001: The case of the East/Japan Sea. Geophys. Res. Lett., *29,* doi:10.1029/2001GL014498.

Kim, K.-R., T. S. Rhee, K. Kim and J. Y. Chung. 1991. Chemical characteristics of the East Sea Intermediate Water in the Ulleung Basin. J. Korean Soc. Oceanogr., *26,* 278–290.

Kim, Y.-G. and K. Kim. 1999. Intermediate waters in the East/Japan Sea. J. Oceanogr., *55,* 123–132.

Lee, C. M., L. N. Thomas and Y. Yoshikawa. 2006. Intermediate water formation at the Japan/East Sea subpolar front. Oceanogr., *19,* 110–121.

Lee, J. C. 1983. Variation of sea level and sea surface temperature associated with wind-induced upwelling in the southeast coast of Korea in summer. J. Korean Soc. Oceanogr., *18,* 149–160.

Lee, J. C. and J. Y. Na. 1985. Structure of upwelling off the southeast coast of Korea. J. Korean Soc. Oceanogr., *20,* 215–228.

Lee, J. C. and W. Chung. 1981. On the seasonal variations of surface current in the eastern sea of Korea. J. Korean Soc. Oceanogr., *16,* 1–11.

Lee, T. and I.-N. Kim. 2003. Chemical imprints of the upwelled waters off the coast of the southern East Sea of Korea. J. Korean Soc. Oceanogr., *38,* 101–110.

Lie, H. J. and Y. H. Seung. 1994. A review on status and development of physical oceanography research in Korea. J. Korean Soc. Oceanogr., *29,* 121–131.

Lim, D. B. and S. D. Chang. 1969. On the cold water mass in the Korea Strait. J. Korean Soc. Oceanogr., *4,* 71–82.

Min, D.-H. 1999. Studies of large-scale intermediate and deep water circulation and ventilation in the North Atlantic, South Indian and Northeast Pacific Oceans, and in the East Sea (Sea of Japan), using chlorofluorocarbons as tracers, Ph.D. Thesis, University of California San Diego, La Jolla. 170 pp.

Min, D.-H. and M. J. Warner. 2005. Basin-wide circulation and ventilation study in the East Sea (Sea of Japan) using chlorofluorocarbon tracers. Deep-Sea Res. II, *52,* 1580–1616.

Min, H. S. and C.-H. Kim. 2006. Water mass formation variability in the intermediate layer of the East Sea. Ocean Sci. J., *41,* 255–260.

Park, C. K. 1978. Chemical oceanographic aspect of the cold water mass in offshore of the east coast of Korea. Bull. Korean Fish. Soc., *11,* 49–54.

Park, G.-H., K. Lee, P. Tishchenko, D.-H. Min, M. J. Warner, L. D. Talley, D.-J. Kang and K.-R. Kim. 2006. Large accumulation of anthropogenic CO_2 in the East (Japan) Sea and its significant impact on carbonate chemistry. Global Biogeochem. Cycl., *20,* GB4013, doi:10.1029/2005GB002676.

Poole, R. and M. Tomczak. 1999. Optimum multiparameter analysis of the water mass structure in the Atlantic Ocean thermocline. Deep-Sea Res. I, *46,* 1895–1921.

Postlethwaite, C. F., E. J. Rohling, W. J. Jenkins and C. F. Walker. 2005. A tracer study of ventilation in the Japan/East Sea. Deep-Sea Res. II, *52,* 1684–1704.

Senjyu, T. 1999. The Japan Sea Intermediate Water; its characteristics and circulation. J. Oceanogr., *55,* 111–122.

Senjyu, T., T. Aramaki, S. Otosaka, O. Togawa, M. Danchenkov, E. Karasev and Y. Volkov. 2002. Renewal of the bottom water after the winter 2000–2001 may spin-up the thermohaline circulation in the Japan Sea. Geophys. Res. Lett., *29,* doi:10.1029/2001GL014093.

Seung, Y. H. 1997. Application of the ventilation theory to the East Sea. J. Korean Soc. Oceanogr., *32,* 8–16.

Seung, Y. H. and K. Kim. 1993. A numerical modeling of the East Sea circulation. J. Korean Soc. Oceanogr., *28,* 292–304.

Seung, Y. H. and K.-J. Kim. 1997. Estimation of the residence time for renewal of the East Sea Intermediate Water using MICOM. J. Korean Soc. Oceanogr., *32,* 17–27.

Shin, C.-W. 2006. The inflow path of the East Sea Intermediate Water into the Ulleung Basin in July 2005. Ocean and Polar Res., *28,* 153–161.

Shin, C.-W., S.-K. Byun, C. Kim, J. H. Lee, B.-C. Kim, S.-C. Hwang, Y. H. Seung and H.-R. Shin. 2007. General characteristics of the East Sea Intermediate Water. Ocean Polar Res., *29,* 33–42.

Shin, C.-W., S.-K. Byun, C. Kim and Y.-H. Seung. 1998. Southward intrusion of the East Sea Intermediate Water into the Ulleung Basin: observations in 1992 and 1993. J. Korean Soc. Oceanogr., *33,* 146–156.

Talley, L. D., V. Lobanov, V. Ponomarev, A. Salyuk, P. Tishchenko, I. Zhabin and S. Riser. 2003. Deep convection and brine rejection in the Japan Sea. Geophys. Res. Lett., *30,* doi:10.1029/2002GL016451.

Talley, L. D., D.-H. Min, V. B. Lobanov, V. A. Luchin, V. I. Ponomarev, A. N. Salyuk, A. Y. Shcherbina, P. Y. Tishchenko and I. Zhabin. 2006. Japan/East Sea water masses and their relation to the sea's circulation. Oceanogr., *19,* 32–49.

Talley, L. D., P. Tischenko, V. Luchin, A. Nedashkovskiy, S. Sagalaev, D.-J. Kang, M. Warner and

D.-H. Min. 2004. Atlas of Japan (East) Sea hydrographic properties in summer, 1999. Prog. Oceanogr., *61,* 277–348.

Tomczak, M. and D. G. B. Large. 1989. Optimum Multiparameter analysis of mixing in the thermocline of the Eastern Indian Ocean. J. Geophys. Res., *94,* 16141–16149.

Tsunogai, S., K. Kawada, S. Watanabe and T. Aramaki. 2003. CFC indicating renewal of the Japan Sea Deep Water in winter 2000–2001. J. Oceanogr., *59,* 685–693.

Uda, M. 1934. The results of simultaneous oceanographical investigations in the Japan Sea and its adjacent waters in May and June, 1932. J. Imp. Fish. Exp. Sta., *5,* 57–190.

Watanabe, T., M. Hirai and H. Yamada. 2001. High-salinity intermediate water of the Japan Sea in the eastern Japan Basin. J. Geophys. Res., *106,* 11437–11450.

Weiss, R. F. 1970. The solubility of nitrogen, oxygen and argon in water and seawater. Deep-Sea Res., *17,* 721–735.

Yang, H.-S., S.-S. Kim, C.-G. Kang and K.-D. Cho. 1991. A study on sea water and ocean current in the sea adjacent to Korea Peninsula III. Chemical characteristics of water masses in the polar front area of the central Korean East Sea. Bull. Korean Fish. Soc., *24,* 185–192.

Yoon, J.-H. 1982. Numerical experiment on the circulation in the Japan Sea Part III. Mechanism of the nearshore branch of the Tsushima Current. J. Oceanogr. Soc. Japan, *38,* 125–130.

Yoon, J.-H. and H. Kawamura. 2002. The formation and circulation of the intermediate water in the Japan Sea. J. Oceanogr., *58,* 197–211.

Yoshikawa, Y., K. Akitomo and T. Awaji. 2001. Formation process of intermediate water in baroclinic current under cooling. J. Geophys. Res., *106,* 1033–1051.

Yoshikawa, Y., T. Awaji and K. Akitomo. 1999. Formation and circulation processes of intermediate water in the Japan Sea. J. Phys. Oceanogr., *29,* 1701–1722.

Received: *9 February, 2010;* revised: *26 December, 2010.*